

Trastuzumab distribution in an *in-vivo* and *in-vitro* model of brain metastases of breast cancer

Tori B. Terrell-Hall¹, Mohamed Ismail Nounou^{2,3}, Fatema El-Amrawy², Jessica I.G. Griffith¹ and Paul R. Lockman¹

¹Department of Basic Pharmaceutical Sciences, School of Pharmacy, West Virginia University HSC, Morgantown, West Virginia 26506, USA

²Department of Pharmaceutics, Faculty of Pharmacy, Alexandria University, Alexandria 21521, Egypt

³Department of Pharmaceutical Sciences, School of Pharmacy, University of Saint Joseph (USJ), Hartford, Connecticut 06103, USA

Correspondence to: Paul R. Lockman, **email:** prlockman@hsc.wvu.edu

Keywords: drug delivery, metastasis, microfluidic device, blood brain barrier, permeability

Received: March 15, 2017

Accepted: July 03, 2017

Published: July 26, 2017

Copyright: Terrell-Hall et al. This is an open-access article distributed under the terms of the Creative Commons Attribution License 3.0 (CC BY 3.0), which permits unrestricted use, distribution, and reproduction in any medium, provided the original author and source are credited.

ABSTRACT

Background: Drug and antibody delivery to brain metastases has been highly debated in the literature. The blood-tumor barrier (BTB) is more permeable than the blood-brain barrier (BBB), and has shown to have highly functioning efflux transporters and barrier properties, which limits delivery of targeted therapies.

Methods: We characterized the permeability of ¹²⁵I-trastuzumab in an *in-vivo*, and fluorescent trastuzumab-Rhodamine123 (t-Rho123) in a novel microfluidic *in-vitro*, BBB and BTB brain metastases of breast cancer model. *In-vivo*: Human MDA-MB-231-HER2+ metastatic breast cancer cells were grown and maintained under static conditions. Cells were harvested at 80% confluency and prepped for intra-cardiac injection into 20 homozygous female Nu/Nu mice. *In-vitro*: In a microfluidic device (SynVivo), human umbilical vein endothelial cells were grown and maintained under shear stress conditions in the outer compartment and co-cultured with CTX-TNA2 rat brain astrocytes (BBB) or Met-1 metastatic HER2+ murine breast cancer cells (BTB), which were maintained in the central compartment under static conditions.

Results: Tissue distribution of ¹²⁵I-trastuzumab revealed only ~3% of injected dose reached normal brain, with ~5% of injected dose reaching brain tumors. No clear correlation was observed between size of metastases and the amount of ¹²⁵I-trastuzumab localized *in-vivo*. This heterogeneity was paralleled *in-vitro*, where the distribution of t-Rho123 from the outer chamber to the central chamber of the microfluidic device was qualitatively and quantitatively analyzed over time. The rate of t-Rho123 linear uptake in the BBB ($0.27 \pm 0.33 \times 10^4$) and BTB ($1.29 \pm 0.93 \times 10^4$) showed to be significantly greater than 0 ($p < 0.05$). The BTB devices showed significant heterogenous tendencies, as seen in *in-vivo*.

Conclusions: This study is one of the first studies to measure antibody movement across the blood-brain and blood-tumor barriers, and demonstrates that, though in small and most likely not efficacious quantities, trastuzumab does cross the blood-brain and blood-tumor barriers.

INTRODUCTION

Brain metastases are a fatal neurological complication of breast cancer which have historically been a major cause of morbidity. Women with symptomatic central nervous system (CNS) metastases have a median survival of approximately 4 months [1]. Furthermore, less than 2% of women survive two years post-diagnosis [2]. The risk of developing brain metastasis has been reported to range from 10 to 16 % among advanced-stage breast cancer patients, making it the second most common cause of metastatic brain tumors after lung cancer (10–25%) [3-7].

Among the many associated risk factors in the development of brain metastases from breast cancer, hormone receptor status is significant [8]. Within the HER2-positive (HER2+) subset, hormone receptor status is associated with CNS relapse. Patients with hormone receptor-negative/HER2+ tumors experience increased risk of the CNS as site of first relapse as compared to patients with hormone receptor-positive/HER2+ tumors [9-12]. Up to 37% of patients with HER2+ breast cancer relapse is associated with intracranial metastases, despite control of the peripheral tumors [13-15]. Palmieri *et al.* demonstrated that HER2 overexpression increases the outgrowth of metastatic tumors cells in the brain in breast carcinoma cell lines [12]. A limiting factor in the treatment of brain metastases is the inability of chemotherapy to reach the desired tumor location. This is due, in large part, to the presence of a strictly controlled and complex vascular network known as the blood-brain barrier (BBB).

The BBB is a physical and functional barrier limiting passive diffusion of extrinsic agents into brain [16-19]. The BBB is mainly composed of endothelial cells, in addition to pericytes, astrocytes and neuronal cells that play an important supportive role in the function of the BBB [20]. The BBB endothelial cells are linked together by tight junction protein complexes, which prevent passive paracellular transport of most water-soluble compounds and many lipid soluble compounds, with the exception of small gaseous compounds like carbon dioxide and molecular water [16, 19-23].

The function and organization of the BBB may be altered under pathological conditions. In the case of tumors, the BBB's structure and integrity are altered, forming the "blood-tumor barrier" (BTB) [22]. The BTB differs from the BBB in its decreased tight junction expression [24], a disruption of the basement membrane [25] and an increase in permeability [26, 27]. However, radiologic data have shown that not all brain metastases display significantly elevated BTB permeability [28]. The changes in BTB vascular permeability are typically heterogeneous throughout the tumor region [29, 30]. It has been observed that brain metastases from HER2+ breast cancers infiltrate brain parenchyma without disrupting the BBB, unlike brain metastases from triple negative or basal-type breast cancers, which often disrupt the BBB [9, 14, 31].

Targeted therapies have modernized cancer treatment, offering an improved therapeutic ratio [32]. These drugs, such as small molecule inhibitors (lapatinib) [33] and monoclonal antibodies and their drug conjugates (mABs) [32], have prolonged progression-free survival and effected some reduction of CNS tumor burden in patients [34-36]. With the advent of these therapies, patients with HER2+ metastatic disease are now living 2-3 years post-diagnosis [36]. However, the ability of these drugs and antibodies to permeate and distribute within the brain and brain metastases has not completely been elucidated. Table 1 details some examples from literature of various antibody and antibody-drug conjugates' permeability to the brain in preclinical models, with or without BBB disruption.

In this work, we have tested the permeability of ¹²⁵I-trastuzumab in an *in-vivo*, and fluorescent trastuzumab-Rho123 (t-Rho123) in a novel *in-vitro* model of brain metastases of breast cancer. This study demonstrates that trastuzumab crosses the BTB and the accumulates in tumor in our preclinical model of brain metastases of breast cancer and is accompanied by confirmatory microfluidic *in-vitro* experiments.

RESULTS

To visualize *in-vitro* movement of t-Rho123, microfluidic BBB and BTB chips (Figure 1A) were established and utilized as previously published [37]. The distribution of t-Rho123 in BBB and BTB models was analyzed. We observed a linear increase of fluorescent trastuzumab uptake in both the BBB ($0.27 \pm 0.33 \times 10^4$) (Figure 1C) and BTB ($1.29 \pm 0.93 \times 10^4$) (Figure 1D) models significantly greater than 0 ($p < 0.05$). The rate of movement of fluorescent trastuzumab was quantified through the addition of a region of interest in the outer chamber (comparative to concentration of drug in plasma, C_{pf}) and a region of interest in the central chamber (comparative to concentration of drug in brain, C_{cc}), then divided by the sum intensity of tracer in the outer chamber ($C_{cc} + C_{pf} / C_{pf}$) and plotted over time. The slope of this line, k_{in} ($\mu\text{L}/\text{min}/\mu\text{m}^2$), was plotted and graphed (Figure 1B) as the mean \pm S.E.M. for the BBB (0.18 ± 0.05 , $n=3$) and BTB (2.12 ± 1.36 , $n=3$) models. Both the k_{in} for the BBB models as well as the heterogeneity of the k_{in} values in the BTB models were comparable to *in-vivo*. The BBB ($p < 0.0033$) and BTB ($p < 0.0005$) models were significantly different in comparison to the unrestricted diffusion k_{in} of this model, as previously described [38].

Organ distribution of ¹²⁵I-trastuzumab after intracardiac injection of 20 Nu/Nu mice with a HER2+ breast cancer cell line was determined. After the mice developed metastases (~32 days post-injection), iodinated-labeled ¹²⁵I-trastuzumab was injected and allowed to circulate, followed by the administration of TRD 10 minutes prior to decapitation. Quantitative autoradiography

Table 1: Examples from literature of various antibody and antibody-drug conjugates' permeability to the brain in preclinical models, with or without BBB disruption

Antibody	Ab use	Drug	Model	Efficacy	Ref.
¹²⁵ I-MAb	Tracer	-	Normal rat brain	Permeability was increased with osmotic BBB disruption.	Neuwelt et al., 1986 [52]
¹²⁵ I-IgG 96.5 ¹²⁵ I-FAb 96.5 ¹²⁵ I-FAb 48.7				<ul style="list-style-type: none"> • Permeability increased with osmotic BBB disruption. • Enhanced & sustained retention of IgG in the brain. 	Neuwelt et al., 1987 [53]
L6 IgG F(Ab') ₂ FAb			LX-1 human small-cell lung carcinoma intracerebral xenograft in nude rat	Antibody permeability to the brain increased with increased delay in dosing	Neuwelt et al., 1994 [54]
L6 IgG-conjugated iron oxine nanoparticles	Imaging (MRI)			Specific antibody displayed specific binding and potential for diagnostic enhancement of MRI	Remsen et al., 1996 [55]
SGN-15 MAb	Therapy	Doxorubicin		Immunoconjugate delivered across the BBB was effective against antigen-positive tumor cells	Neuwelt et al., 2003 [56]
Bevacizumab		Carboplatin	UW28 human glioma xenografts in nude rats	Combination therapy of Bevacizumab with carboplatin was more effective than Bevacizumab alone.	Jahnke et al., 2009 [57]
Rituximab Anti-CD20	Therapy & Imaging (MRI)	Rituximab anti-CD20	Lymphoma rat model	Rituximab was effective at decreasing tumor volume and improving survival rate in a CNS lymphoma model	Muldoon et al., 2011 [58]
TDM1	Therapy	Emantsine	Her2+ BT474 or MDA-MB-361 CNS metastases in nude mice	TDM1 displayed increased survival rate in comparison to trastuzumab	Askoxylakis et al., 2015 [46]
⁸⁹ Zr-trastuzumab muMAb 4D5 TDM1	Tracer & Therapy	Emantsine	HER2-expressing transgenic Fo2-1282 or Fo5 mouse breast cancer in mice	<ul style="list-style-type: none"> • Trastuzumab displayed preferential uptake in tumor lesions • muMAb 4D5 and TDM1 significantly increased survival, as did combination therapy with PI3K/mTOR inhibitor GNE-317 	Phillips et al., 2017 [59]

(QAR) was used to measure the brain tissue distribution of ¹²⁵I-trastuzumab. Figure 2A represents organ distribution of ¹²⁵I-trastuzumab, variability in different body organs is observed. ¹²⁵I-trastuzumab was found in significant quantities in spleen (5.04%, SD= 3.91), lungs (4.45%, SD=

2.08), liver (3.54%, SD= 2.26), kidney (3.12 %, SD= 2.06), and heart (3.08%, SD= 1.78) compared to normal brain (0.30%, SD= 0.22) and tumor brain tissues (0.46%, SD= 0.46). The accumulation of ¹²⁵I-trastuzumab in tumor brain

was 1.5 fold higher than normal brain tissue ($p < 0.0001$) (Figure 2B).

Heterogeneous and limited distribution of ^{125}I -trastuzumab in our preclinical brain metastases of breast cancer model is shown in Figure 3A-3C. Metastases were categorized into four groups based upon the magnitude of permeability change compared to normal brain, where low, intermediate, medium and high corresponds to the following: $< \text{mean brain} + 3\text{xSD}$; $> \text{mean brain} + 3\text{xSD}$ but < 2 fold; 2-4 fold; > 4 fold, respectively. The mean and standard deviation of the four groups were, 1.30 and 0.34 for low permeability, 1.88 and 0.07 for intermediate permeability, 2.79 and 0.61 for medium permeability, and 7.40 and 4.66 for high permeability (Figure 3D).

Fold increase in ^{125}I -trastuzumab (over normal brain) was plotted versus metastasis size (mm^2) in individual 231-Br-HER2 brain metastases (Figure 3E). No clear correlation was found between the size of brain metastases and the amount of ^{125}I -trastuzumab localized within the tumor region (Figure 3E). K_{in} values were determined separately for normal and tumor areas of the brain (Figure 3F). Mean k_{in} for normal brain tissue was $1.457 \times 10^7 \text{ mL/}$

sec/g ($\text{SD} = 0.55$) while mean k_{in} in the case of tumor brain was 3.80 mL/sec/g ($\text{SD} = 2.17$).

DISCUSSION

Treatment of brain metastases of breast cancer conventionally consists of surgery, whole brain radiation, stereotactic radiosurgery, chemotherapy, and/or biological therapies [39]. Various chemotherapeutic agents have shown only a modest effect on survival due to their limited ability to cross the BBB [39]. In a preclinical study using two different models of brain metastases of breast cancer, most metastases exhibited some increased BTB permeability in comparison to normal brain. However, BTB permeability remained poorly correlated with lesion size, and only approximately 10% of lesions with the highest permeability exhibited cytotoxic responses to paclitaxel or doxorubicin [29]. In low-grade gliomas, the BTB resembles a normal functioning BBB, while in high-grade gliomas, BTB is disrupted “leaky”, as it is characterized by major alterations of the normal vascular function, shown through contrast-enhanced MRI [22,

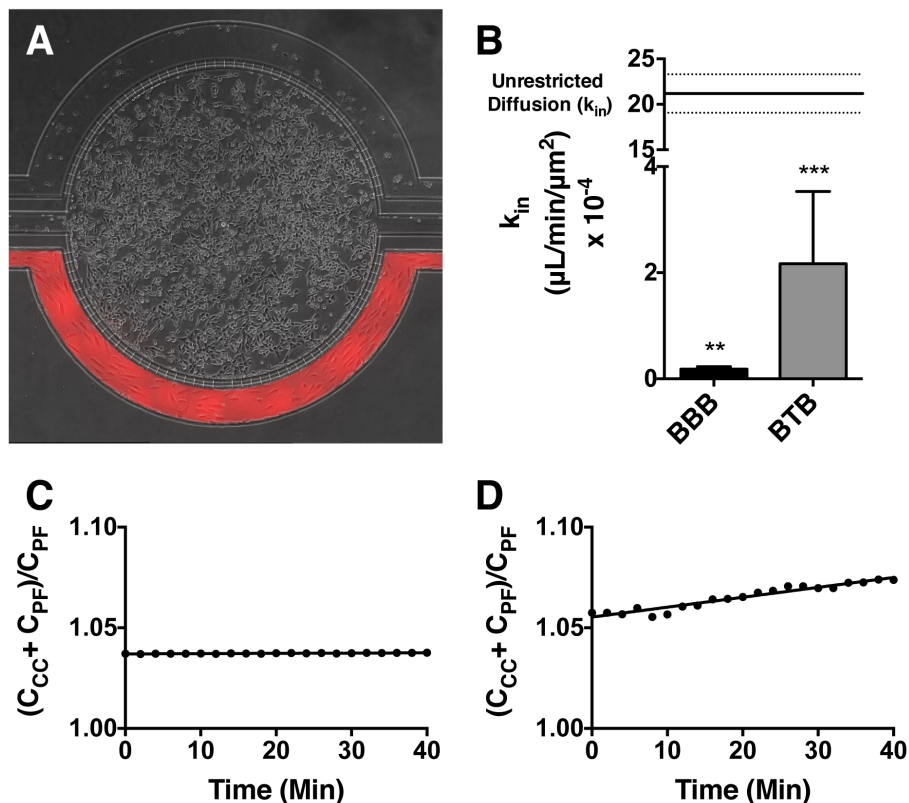


Figure 1: Mechanism of trastuzumab movement. Linear central compartment accumulation of t-Rho123 in *in-vitro* BBB and BTB microfluidic chip models. Representative image of model with TRITC labeled t-Rho123 flowing over HUVEC cells in the outer compartment and either astrocytes or JIMT-1 cancer cells in the central compartment (A). Rate of t-Rho123 movement in each model plotted against the unrestricted diffusion k_{in} ; ** $p < 0.0033$ significance between BBB model and unrestricted diffusion k_{in} , $n = 3$; *** $p < 0.0005$ significance between BTB model and unrestricted diffusion k_{in} , $n = 3$. All data represent mean \pm S.E.M. Each model is significantly different than 0 ($p < 0.05$) (B). Representative graphs of the rate of accumulation of t-Rho123 in the BBB (C) and BTB (D) microfluidic devices ($n \geq 3$).

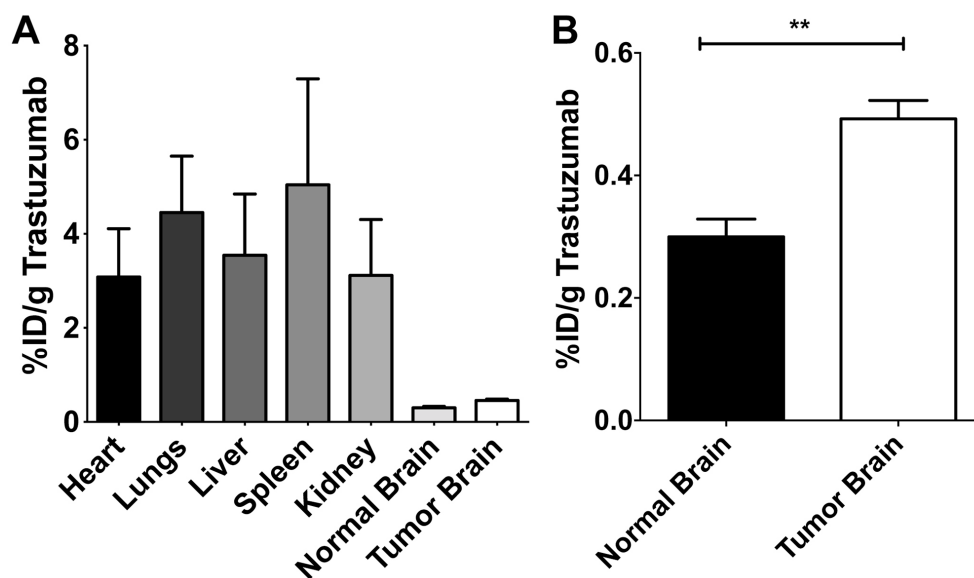


Figure 2: The distribution of radiolabeled ^{125}I -trastuzumab in various body organs (A) and in normal and tumor brain tissues (B). “%ID/g” refers to the percentage of injected dose of ^{125}I -trastuzumab per gram of tissue.

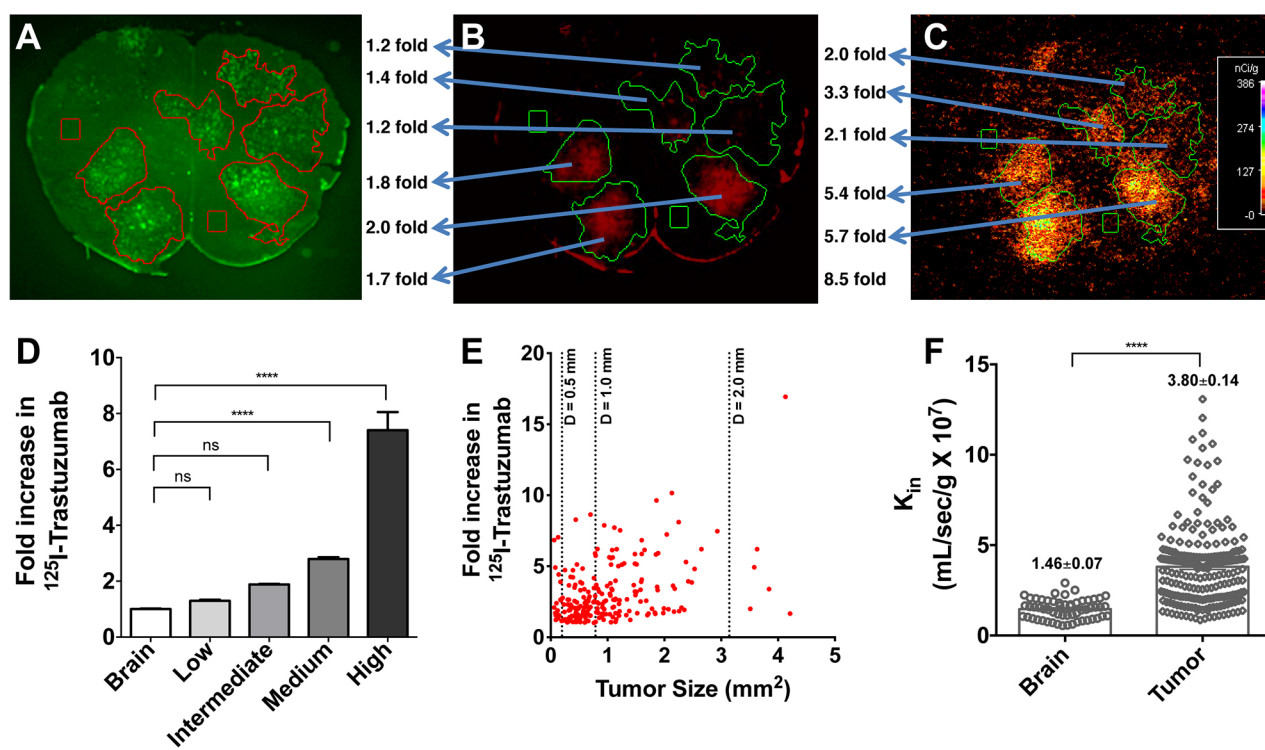


Figure 3: Heterogeneous and limited distribution of ^{125}I -trastuzumab in preclinical brain metastases of breast cancer model. Representative images of location of eGFP labeled 231-Br-Her2 brain metastases (A) and brain accumulation of Texas Red 625 Da (B) and ^{125}I -trastuzumab (C) are shown. Metastases were categorized into four groups based upon the magnitude of permeability change compared to normal brain, where low, intermediate and high corresponds to the following: $< \text{mean brain} + 3\text{xSD}$; $> \text{mean brain} + 3\text{xSD}$ but < 2 fold; $2-4$ fold; > 4 fold, respectively (values represent mean \pm SD, $n=251$ metastases) (D). Fold increase in ^{125}I -trastuzumab (over normal brain) was plotted versus metastasis size (mm^2) in individual 231-Br-Her2 brain metastases. Metastases size was calculated based on tumor(s) surface area generated from the fluorescent tumor lesions in brain slices (3A) and reported in mm^2 (E). The correlation was minimal with ^{125}I -trastuzumab fold increase versus lesion size. k_{in} values for normal and tumor areas of the brain (F). At least, 20 slides/animal/group were analyzed in each study.

40]. However, the magnitude of this local disruption may or may not be sufficient to allow drug penetration in meaningful quantities, and is thus considered a major obstacle for drug delivery to the brain [41].

Trastuzumab (Herceptin[®], Genentech/ Roche), is a widely used humanized mAB for the treatment of HER2+ breast cancer due to its ability to recognize and bind to the extracellular juxtamembrane domain of HER2. Through this binding, trastuzumab is able to inhibit the proliferation, and therefore survival, of HER2-dependent tumors [7]. The ability of trastuzumab to significantly cross the BBB is unclear [42]. Şendur *et al.* [43] reported a case study using a combination of lapatinib and capecitabine followed by trastuzumab in HER2+ brain metastatic breast cancer. No progression of cranial metastases was found post-treatment. In another case series by Mutlu *et al.* [44], one in three patients with HER2+ breast cancer brain metastasis maintained the brain metastases post-treatment with a combination of weekly trastuzumab plus vinorelbine, however, these studies do not necessarily indicate the effectiveness of trastuzumab alone. In an *in-vivo* study by Kodack *et al.*, it was observed that through the use of a combination of a HER2 inhibitor with an anti-VEGF receptor-2 antibody, trastuzumab, and lapatinib, tumor growth was significantly slowed in the brain, resulting in increased survival in a mouse model of HER2-amplified breast cancer brain metastasis using an orthotopic xenograft of BT474 cells [45].

An antibody-drug conjugate of trastuzumab, trastuzumab-emansine (TDM1), has displayed very promising efficacy in preclinical and clinical trials in CNS metastases [34, 46]. However, in patients without brain metastases, the ratio of trastuzumab in plasma to trastuzumab in cerebrospinal fluid is > 300:1 [47]. Other several studies highlighted the ability of mABs to reach brain metastases in numerous animal models such as blood-borne tumor from outside the brain, and dormant tumor that grows enough to rupture the BBB, and thus allow mABs to infiltrate [48]. In addition to physical barriers, several functional barriers contribute to the restrictive nature of BBB, which represents a major obstacle to effective drug delivery into the CNS [49]. Future studies should address how these antibodies and drug conjugates display such efficacy in control of CNS tumor burden while movement of antibodies across the BBB is still restricted. Another method for improving treatment, which is currently under investigation, is selectively altering BTB permeability to increase antibody delivery to CNS lesions.

MATERIALS AND METHODS

In-vitro studies

Chemicals and reagents

Texas Red 70,000 MW Dextran (TRD 70 kDa) was purchased from Molecular Probes (Invitrogen, Carlsbad, CA). Trastuzumab (Herceptin[®], Genentech/ Roche) was buffer-exchanged into 50 mM potassium phosphate buffer and 150 mM sodium chloride adjusted to pH of 6.7. Trastuzumab was fluorescently linked to Rhodamine-123 (Innova Biosciences, Babraham, England). All other chemicals were of analytical grade and purchased from Sigma-Aldrich (St. Louis, MO).

Cell culture for *in-vitro* studies

Human Umbilical Vein Endothelial Cells (HUVECs) were purchased from Lonza (Allendale, NJ). CTX-TNA2 rat brain astrocyte cell line was generously provided by the laboratory of Dr. Jim Simpkins (West Virginia University, Morgantown, WV). Both HUVEC and astrocyte line were cultured and maintained in Endothelial Basal Medium – 2 (EBM-2) with the supplementation of EGM-2 Bullet Kits from Lonza (Allendale, NJ). The laboratory of Dr. Patricia Steeg, of the National Cancer Institute, generously provided a JIMT-1 brain metastases of breast cancer cell line, a line which naturally overexpresses HER2. These cells were cultured and maintained in DMEM supplemented with 10% Fetal bovine serum and 1% penstrep. All cell lines for *in-vitro* studies were grown within a 37°C humidified incubator with 5% CO₂ until ~85-90% confluent.

Cell culture in microfluidic chip

The co-culture idealized microvascular microfluidic chips used in this study were obtained from SynVivo Inc (Huntsville, AL). These microfluidic chips were prepared, then cultured with cells and maintained as previously described [37, 38].

Transport studies and quantification using fluorescent microscopy

For each device, a BD Leur-lok syringe connected to Tygon tubing was filled with EBM-2 media containing fluorescent trastuzumab. This syringe was then mounted on a programmable Harvard PHD 2000 syringe pump (Harvard Apparatus, Holliston, MA) and tubing was inserted into the device. Chips were maintained at 37°C with 5% CO₂ and mounted in an automated stage enclosure on a Nikon Eclipse TE2000-E Live Cell Sweptfield Confocal microscope (Melville, NY). Permeability was measured through the perfusion of fluorescently labeled trastuzumab through the outer chamber at 0.1 µL/min. Brightfield (25 ms exposure) and TRITC (200 ms exposure) images were acquired every two minutes for 90 minutes with a Photometrics CoolSnap HQ2 Monochrome CCD Camera (Tucson, AZ) with a 20x/0.75 Plan Fluor

Phase Contrast objective, having a total field of 6x8 and stitching those images using brightfield with a 10% overlay. Following acquisition, NIS Elements Imaging Software was used to determine Regions of Interest (ROI) and data exported to Prism 6.0. A line of best fit was determined using linear regression (Prism 6.0), and the slope represents the relative rate of accumulation of fluorescence (k_{in}) in the central chamber (representing drug concentration found in normal brain) divided by the amount of fluorescence in the outer chamber (representing drug concentration found in the BBB/BTB vasculature). Unless otherwise noted, data are presented as mean \pm S.E.M.

Kinetic analysis

Unidirectional uptake transfer constants (k_{in}) were calculated using the following equation:

$$(C_{CC} + C_{PF}) / C_{PF} = k_{in}(t) + O_c \quad (\text{Equation 1})$$

Where C_{CC} is the sum intensity of fluorophore in the region of interest in the central compartment (au) at the end of perfusion, C_{PF} is the sum intensity of fluorophore (au) in the region of interest within the outer compartment, t is the perfusion time in minutes from the time the device reached steady state, and O_c is the calculated intercept ($T = 0$ min; “outer compartment volume” (au)). Since the device took 22 minutes to reach steady state, $t=0$ minutes is 22 minutes after start of the experiment and 0 minutes from the start of steady state. After the determination of a perfusion time where an adequate amount of fluorescent marker was allowed to pass into brain while still remaining in the linear uptake zone, k_{in} was determined [50, 51].

Statistical analysis

Using linear regression with best-fit values, the slope of the line (k_{in}) was determined. One-way ANOVA analysis, unpaired student t test's with Welch's correction, and an F test to compare variances were used for the comparison of k_{in} values between the unrestricted diffusions, BBB, and BTB models. For all data, errors are reported as standard error of the mean unless otherwise indicated. Differences were considered statistically significant at $p < 0.05$. (GraphPad Prism version 6.00 for Mac, GraphPad Software, San Diego, CA, USA).

In-vivo studies

Chemicals and reagents

Texas red conjugated 625 MW dextran (TRD 625 Da) was purchased from Molecular Probes (Invitrogen, Carlsbad, CA). Trastuzumab (Roche) was buffer-exchanged into 50 mM potassium phosphate buffer and 150 mM sodium chloride adjusted to pH of 6.7. Trastuzumab was radiolabeled with ^{125}I . All other chemicals were of analytical grade and purchased from Sigma-Aldrich (St. Louis, MO).

Cell culture

Human MDA-MB-231-HER2+ metastatic breast cancer cells expressing enhanced green fluorescent protein (eGFP) and the luciferase construct were cultured in DMEM supplemented with 10% fetal bovine serum and zeocin (300 μ g/ml). Cells were harvested at 80% confluency for intracardiac injection. All cell lines were generously provided by the laboratory of Dr. Patricia Steeg at the National Cancer Institute.

Experimental brain metastases model

Homozygous Female Nu/Nu ($n=20$) mice were obtained from Charles River Laboratories (Kingston, NY) and used for all experiments in this study. All animals were 6–8 weeks of age at the initiation of the metastases models and were housed in a barrier facility. All studies were approved by the Animal Care and Use Committee at Texas Tech University Health Sciences Center and conducted in accordance with the 1996 NIH Guide for the Care and Use of Laboratory Animals. Mice were anesthetized with 2% isoflurane and inoculated with 175,000 breast cancer cells in the left cardiac ventricle with the aid of a stereotaxic device (Stoelting, Wood Dale, IL). In this model, previously validated, the inoculum circulates in the peripheral vasculature, arrests in brain capillaries, extravasates across the blood-brain barrier (BBB), and mice develop metastatic lesions predominantly in the brain [29]. After intracardiac injection, mice were placed in a warmed (37 $^{\circ}$ C) sterile cage and their vitals monitored until fully recovered. Metastases were allowed to develop and visualized with bioluminescent imaging, until neurologic symptoms appeared (\sim 32 days). Animals were then anesthetized with ketamine/xylazine (100 and 8 mg/kg respectively) prior to injection with ^{125}I -trastuzumab via IV bolus dose (femoral vein). ^{125}I -trastuzumab was allowed to circulate for 24h. TRD 625 Da was injected intravenously (femoral vein), and 10 minutes post-injection, blood samples were obtained. Mice were euthanized via decapitation.

Harvesting of the brain and other tissues and organs

Animals were euthanized, and brain tissue was rapidly removed (less than 60 seconds) and placed in isopentane (-65° C). Brains were sliced (20 μ m) using a cryostat (Leica Microsystems, Wetzlar, Germany), and sections were mounted on charged gold plated glass slides, air dried, and stored at -80° C. In addition to the brain, blood and samples from other organs (heart, lungs, liver, spleen, kidney) were collected, washed, and weighed for comparative analysis. Radioactivity was measured immediately following collection (Tri-CARB 2900TR, Perkin Elmer) and expressed as cpm/mg then converted to nCi/g. Distribution ratios are expressed as the amount of radioactivity in the tissue/blood normalized by weight.

Quantitative autoradiography (QAR)

Slides were placed in QAR cassettes (FujiFilm Life Sciences, Stamford, CT) along with ^{125}I autoradiographic standards (Amersham Biosciences). A phosphor screen (FujiFilm Life Sciences, 20×40 super-resolution) was placed on the slides and standards and allowed to develop for up to 14 days. QAR phosphor screens were developed in a high-resolution phosphor-imager (FUJI FLA-7000, FujiFilm Life Sciences) and converted to digital images. Digital QAR images were calibrated to ^{125}I standards and analyzed using MCID Analysis software (InterFocus Imaging LTD, Linton, Cambridge, England). Metastases permeability fold-changes were calculated based on ^{125}I signal intensity within confirmed metastases locations (determined by eGFP fluorescence image overlays) relative to ^{125}I signal intensity in normal brain.

Fluorescence measurement

Texas red fluorescence was imaged using a DsRed sputter filter (excitation/band λ 545/25 nm, emission/band λ 605/70 nm and dichromatic mirror at λ 565 nm) (Chroma Technologies, Bellows Falls, VT) and eGFP (expressed in MDA-MB-231BR-HER2+) using an ET-GFP sputter filter (excitation/band λ 470/40 nm, emission/band λ 525/50 nm and dichromatic mirror at λ 495 nm) (Chroma Technologies, Bellows Falls, VT). Fluorescence image capture and analysis software (SlideBook 5.0; Intelligent Imaging Innovations Inc., Denver, CO) was used to obtain and quantify fluorescence images. Texas red permeability fold-changes were determined by Texas Red Sum intensity (SI) per unit area of metastases relative to the SI per area of contralateral normal brain regions. If metastases occurred in contralateral regions, adjacent slices containing unaffected tissues of the same brain structure were used as comparative normal brain regions. Tumor area was calculated from regions of interest drawn around each lesion and is reported in mm^2 .

Unidirectional uptake transfer constants (k_{in})

All k_{in} values were then calculated from brain distribution volume versus time as previously described [29].

Bioluminescent imaging

Mice were injected with D-luciferin potassium salt (150mg/kg; PerkinElmer, Waltham, MA) dissolved in sterile 1X PBS via intraperitoneal (IP) injection and then anesthetized with 2% isoflurane. Fifteen minutes after IP injection of D-luciferin, darkfield images of mice were acquired with an IVIS Lumineer XV (PerkinElmer) to detect bioluminescence. Animals were imaged 1, 3, 6, 9, 12, 24, 48, 72, 96, 120, 144, and 168 hours post intracardiac injection to ensure successful tumor injection and growth.

Data analysis

Statistical significance was determined by Student's t-test and one-way ANOVA followed by Bonferroni's

multiple comparison's tests. All differences were considered statistically significant at $p < 0.05$. *In-vivo* data is reported as Mean \pm Standard Deviation (SD) unless otherwise noted (GraphPad Prism 7.0, San Diego, CA). Results associated with drug concentration in tumor and brain distant to tumor (BDT) are Mean values of combined readings from all tumor and BDT areas in the study group, without separation by individual animal data. In the case of k_{in} analysis [29], values obtained at individual time points were also pooled together.

CONCLUSIONS

This model has been previously used to observe small molecule movement and P-glycoprotein efflux [38]. We observed a relatively similar fold increase of trastuzumab *in-vivo* as compared to the *in-vitro* observation in the microfluidic device when comparing fold increases from the BBB to the (BTB). The prediction and evaluation of the ability of various therapeutic and diagnostic moieties to cross the BBB and BTB as well as their brain uptake kinetics are critical to progress efficient brain metastases therapy and diagnosis from basic to translational research. Such knowledge is needed for the early detection and management of high-risk brain metastases in patients. This study demonstrates that, trastuzumab does cross the blood-brain and blood-tumor barriers though probably below efficacious concentrations.

Abbreviations

BBB, blood-brain barrier
BTB, blood-tumor barrier
CNS, central nervous system
HER2, human epidermal growth factor receptor-2
mAB, monoclonal antibody
QAR, quantitative autoradiography
SI, sum intensity
t-Rho123, trastuzumab-Rhodamine123

Author contributions

TTH (tbterrell@mix.wvu.edu): participated in the design of the study, performed all of the experiments, as well as data processing and analysis, interpretation of data, statistical analysis, and manuscript drafting, revision, and finalizing.

MIN (nounou@usj.edu): participated in all *in-vivo* experiments, interpretation of data and statistical analysis of *in-vivo* data, and contributed to manuscript drafting, revision, and finalizing.

FEA (fatema.el.amrawy@gmail.com): contributed to manuscript drafting, revision, and finalizing.

JG (jgriff30@mix.wvu.edu): contributed data processing and analysis as well as manuscript revision and finalizing.

PRL (prlockman@hsc.wvu.edu): conceived and designed the study, and contributed to data processing and analysis, interpretation of data, statistical analysis, and manuscript drafting, revision, and finalizing. All authors read and approved the final manuscript.

ACKNOWLEDGMENTS

The authors would like to thank Ashley Smith (Kiyatec Inc., Greenville, S) and Dr. Prabhakar Pandian (CFDRC, Huntsville, AL) for their patience and expertise in the troubleshooting the microfluidic devices

CONFLICTS OF INTEREST

The authors declare that they have no competing interests.

FUNDING

This research was supported by grants from the National Cancer Institute (R01CA166067-01A1) awarded to P. Lockman. Additional support for this research was provided by WVCTSI through the National Institute of General Medical Sciences of the National Institutes of Health (U54GM104942).

DISCLOSURES AND ETHICS

As a requirement of publication author(s) have provided to the publisher signed confirmation of compliance with legal and ethical obligations including but not limited to the following: authorship and contributions, conflicts of interest, privacy and confidentiality and (where applicable) protection of human and animal research subjects. The authors have read and confirmed their agreement with the ICMJE authorship and conflict of interest criteria. The authors have also confirmed that this article is unique and not under consideration or published in any other publication, and that they have permission from rights holders to reproduce any copyrighted material. Any disclosures are made in this section. The external blind peer reviewers report no conflicts of interest.

REFERENCES

1. Colzani E, Liljegren A, Johansson AL, Adolfsson J, Hellborg H, Hall PF, Czene K. Prognosis of patients with breast cancer: causes of death and effects of time since diagnosis, age, and tumor characteristics. *J Clin Oncol*. 2011; 29:4014-4021.
2. Zimm S, Wampler GL, Stablein D, Hazra T, Young HF. Intracerebral metastases in solid-tumor patients: natural history and results of treatment. *Cancer*. 1981; 48:384-394.
3. Lin NU. Breast cancer brain metastases: new directions in systemic therapy. *Ecancermedalscience*. 2013; 7:307.
4. Palmieri D, Smith QR, Lockman PR, Bronder J, Gril B, Chambers AF, Weil RJ, Steeg PS. Brain metastases of breast cancer. *Breast Dis*. 2006; 26:139-147.
5. Yeh RH, Yu JC, Chu CH, Ho CL, Kao HW, Liao GS, Chen HW, Kao WY, Yu CP, Chao TY, Dai MS. Distinct MR imaging features of triple-negative breast cancer with brain metastasis. *J Neuroimaging*. 2015; 25:474-481.
6. Steeg PS, Camphausen KA, Smith QR. Brain metastases as preventive and therapeutic targets. *Nat Rev Cancer*. 2011; 11:352-363.
7. Park YH, Park MJ, Ji SH, Yi SY, Lim DH, Nam DH, Lee JI, Park W, Choi DH, Huh SJ, Ahn JS, Kang WK, Park K, Im YH. Trastuzumab treatment improves brain metastasis outcomes through control and durable prolongation of systemic extracranial disease in HER2-overexpressing breast cancer patients. *Br J Cancer*. 2009; 100:894-900.
8. Sanchez-Munoz A, Plata-Fernandez Y, Fernandez M, Jaen-Morago A, Fernandez-Navarro M, de la Torre-Cabrera C, Ramirez-Tortosa C, Pascual J, Alba E, Sanchez-Rovira P. Tumor histological subtyping determined by hormone receptors and HER2 status defines different pathological complete response and outcome to dose-dense neoadjuvant chemotherapy in breast cancer patients. *Clin Transl Oncol*. 2013.
9. Vaz-Luis I, Ottesen RA, Hughes ME, Marcom PK, Moy B, Rugo HS, Theriault RL, Wilson J, Niland JC, Weeks JC, Lin NU. Impact of hormone receptor status on patterns of recurrence and clinical outcomes among patients with human epidermal growth factor-2-positive breast cancer in the National Comprehensive Cancer Network: a prospective cohort study. *Breast Cancer Res*. 2012; 14:R129.
10. Bendell JC, Domchek SM, Burstein HJ, Harris L, Younger J, Kuter I, Bunnell C, Rue M, Gelman R, Winer E. Central nervous system metastases in women who receive trastuzumab-based therapy for metastatic breast carcinoma. *Cancer*. 2003; 97:2972-2977.
11. Leyland-Jones B. Human epidermal growth factor receptor 2-positive breast cancer and central nervous system metastases. *J Clin Oncol*. 2009; 27:5278-5286.
12. Palmieri D, Bronder JL, Herring JM, Yoneda T, Weil RJ, Stark AM, Kurek R, Vega-Valle E, Feigenbaum L, Halverson D, Vortmeyer AO, Steinberg SM, Aldape K, Steeg PS. Her-2 overexpression increases the metastatic outgrowth of breast cancer cells in the brain. *Cancer Res*. 2007; 67:4190-4198.
13. Clayton AJ, Danson S, Jolly S, Ryder WDJ, Burt PA, Stewart AL, Wilkinson PM, Welch RS, Magee B, Wilson G, Howell A, Wardley AM. Incidence of cerebral metastases in patients treated with trastuzumab for metastatic breast cancer. *Br J Cancer*. 2004; 91:639-643.

14. Witzel I, Oliveira-Ferrer L, Pantel K, Muller V, Wikman H. Breast cancer brain metastases: biology and new clinical perspectives. *Breast Cancer Res.* 2016; 18:8.
15. Brufsky AM, Mayer M, Rugo HS, Kaufman PA, Tan-Chiu E, Tripathy D, Tudor IC, Wang LI, Brammer MG, Shing M, Yood MU, Yardley DA. Central nervous system metastases in patients with HER2-positive metastatic breast cancer: incidence, treatment, and survival in patients from registHER. *Clin Cancer Res.* 2011; 17:4834-4843.
16. Ballabh P, Braun A, Nedergaard M. The blood-brain barrier: an overview: structure, regulation, and clinical implications. *Neurobiol Dis.* 2004; 16:1-13.
17. Cook LJ, Freedman J. (2011). *Brain Tumors*: Rosen Pub.
18. Dauchy S, Miller F, Couraud PO, Weaver RJ, Weksler B, Romero IA, Scherrmann JM, De Waziers I, Decleves X. Expression and transcriptional regulation of ABC transporters and cytochromes P450 in hCMEC/D3 human cerebral microvascular endothelial cells. *Biochem Pharmacol.* 2009; 77:897-909.
19. Abbott NJ, Patabendige AA, Dolman DE, Yusof SR, Begley DJ. Structure and function of the blood-brain barrier. *Neurobiol Dis.* 2010; 37:13-25.
20. Rip J, Schenk GJ, de Boer AG. Differential receptor-mediated drug targeting to the diseased brain. *Expert Opin Drug Deliv.* 2009; 6:227-237.
21. Abbott NJ, Friedman A. Overview and introduction: the blood-brain barrier in health and disease. *Epilepsia.* 2012; 53:1-6.
22. van Tellingen O, Yetkin-Arik B, de Gooijer MC, Wesseling P, Wurdinger T, de Vries HE. Overcoming the blood-brain tumor barrier for effective glioblastoma treatment. *Drug Resist Updat.* 2015; 19:1-12.
23. Hawkins BT, Davis TP. The blood-brain barrier/neurovascular unit in health and disease. *Pharmacol Rev.* 2005; 57:173-185.
24. Liebner S, Fischmann A, Rascher G, Duffner F, Grote EH, Kalbacher H, Wolburg H. Claudin-1 and claudin-5 expression and tight junction morphology are altered in blood vessels of human glioblastoma multiforme. *Acta Neuropathol.* 2000; 100:323-331.
25. Deo AK, Theil FP, Nicolas JM. Confounding parameters in preclinical assessment of blood-brain barrier permeation: an overview with emphasis on species differences and effect of disease states. *Mol Pharm.* 2013; 10:1581-1595.
26. Tate MC, Aghi MK. Biology of angiogenesis and invasion in glioma. *Neurotherapeutics.* 2009; 6:447-457.
27. Puhalla S, Elmquist W, Freyer D, Kleinberg L, Adkins C, Lockman P, McGregor J, Muldoon L, Nesbit G, Peereboom D, Smith Q, Walker S, Neuwelt E. Unsacredifying the sanctuary: challenges and opportunities with brain metastases. *Neuro Oncol.* 2015; 17:639-651.
28. Lin NU, Bellon JR, Winer EP. CNS metastases in breast cancer. *J Clin Oncol.* 2004; 22:3608-3617.
29. Lockman PR, Mittapalli RK, Taskar KS, Rudraraju V, Gril B, Bohn KA, Adkins CE, Roberts A, Thorsheim HR, Gaasch JA, Huang S, Palmieri D, Steeg PS, Smith QR. Heterogeneous blood-tumor barrier permeability determines drug efficacy in experimental brain metastases of breast cancer. *Clin Cancer Res.* 2010; 16:5664-5678.
30. Villanueva MT. Drug therapy: smuggling trastuzumab into the brain. *Nat Rev Clin Oncol.* 2013; 10:669-669.
31. Yonemori K, Tsuta K, Ono M, Shimizu C, Hirakawa A, Hasegawa T, Hatanaka Y, Narita Y, Shibui S, Fujiwara Y. Disruption of the blood brain barrier by brain metastases of triple-negative and basal-type breast cancer but not HER2/neu-positive breast cancer. *Cancer.* 2010; 116:302-308.
32. Boskovitz A, Wikstrand CJ, Kuan CT, Zalutsky MR, Reardon DA, Bigner DD. Monoclonal antibodies for brain tumour treatment. *Expert Opin Biol Ther.* 2004; 4:1453-1471.
33. Hoelder S, Clarke PA, Workman P. Discovery of small molecule cancer drugs: successes, challenges and opportunities. *Mol Oncol.* 2012; 6:155-176.
34. Keith KC, Lee Y, Ewend MG, Zagar TM, Anders CK. Activity of trastuzumab-emtansine (Tdm1) in Her2-positive breast cancer brain metastases: a case series. *Cancer Treat Commun.* 2016; 7:43-46.
35. Murthy P, Kidwell KM, Schott AF, Merajver SD, Griggs JJ, Smerage JD, Van Poznak CH, Wicha MS, Hayes DF, Henry NL. Clinical predictors of long-term survival in HER2-positive metastatic breast cancer. *Breast Cancer Res Treat.* 2016; 155:589-595.
36. Olson EM, Najita JS, Sohl J, Arnaut A, Burstein HJ, Winer EP, Lin NU. Clinical outcomes and treatment practice patterns of patients with HER2-positive metastatic breast cancer in the post-trastuzumab era. *Breast.* 2013; 22:525-531.
37. Prabhakarandian B, Shen MC, Nichols JB, Mills IR, Sidoryk-Wegrzynowicz M, Aschner M, Pant K. Sym-BBB: a microfluidic Blood Brain Barrier model. *Lab Chip.* 2013; 13:1093-1101.
38. Terrell-Hall TB, Ammer AG, Griffith JI, Lockman PR. Permeability across a novel microfluidic blood-tumor barrier model. *Fluids Barriers CNS.* 2017; 14:3. <https://doi.org/10.1186/s12987-017-0050-9>.
39. Rostami R, Mittal S, Rostami P, Tavassoli F, Jabbari B. Brain metastasis in breast cancer: a comprehensive literature review. *J Neurooncol.* 2016.
40. Dhermain FG, Hau P, Lanfermann H, Jacobs AH, van den Bent MJ. Advanced MRI and PET imaging for assessment of treatment response in patients with gliomas. *Lancet Neurol.* 2010; 9:906-920.
41. Tzeng SY, Green JJ. Therapeutic nanomedicine for brain cancer. *Ther Deliv.* 2013; 4:687-704.
42. Kute T, Lack CM, Willingham M, Bishwokama B, Williams H, Barrett K, Mitchell T, Vaughn JP. Development of

- Herceptin resistance in breast cancer cells. *Cytometry A*. 2004; 57:86-93.
43. Sendur MA, Uncu D, Zengin N. Longest progression-free survival with lapatinib and capecitabine combination followed by trastuzumab in HER2-positive brain metastatic breast cancer. *Med Oncol*. 2014; 31:890.
 44. Mutlu H, Buyukcelik A. The combination of weekly trastuzumab plus vinorelbine may be preferable regimen in HER-2 positive breast cancer patients with brain metastasis. *J Oncol Pharm Pract*. 2015; 21:310-312.
 45. Kodack DP, Chung E, Yamashita H, Incio J, Duyverman AM, Song Y, Farrar CT, Huang Y, Ager E, Kamoun W, Goel S, Snuderl M, Lussiez A, et al. Combined targeting of HER2 and VEGFR2 for effective treatment of HER2-amplified breast cancer brain metastases. *Proc Natl Acad Sci U S A*. 2012; 109:E3119-3127.
 46. Askoxylakis V, Ferraro GB, Kodack DP, Badeaux M, Shankaraiah RC, Seano G, Kloepper J, Vardam T, Martin JD, Naxerova K, Bezwada D, Qi X, Selig MK, et al. Preclinical efficacy of ado-trastuzumab emtansine in the brain microenvironment. *J Natl Cancer Inst*. 2016; 108.
 47. Pestalozzi BC, Brignoli S. Trastuzumab in CSF. *J Clin Oncol*. 2000; 18:2349-2351.
 48. Lampson LA. Monoclonal antibodies in neuro-oncology: getting past the blood-brain barrier. *MAbs*. 2011; 3:153-160.
 49. Deeken JF, Loscher W. The blood-brain barrier and cancer: transporters, treatment, and Trojan horses. *Clin Cancer Res*. 2007; 13:1663-1674.
 50. Smith QR, Takasato Y. Kinetics of amino acid transport at the blood-brain barrier studied using an in situ brain perfusion technique. *Ann N Y Acad Sci*. 1986; 481:186-201.
 51. Takasato Y, Rapoport SI, Smith QR. An in situ brain perfusion technique to study cerebrovascular transport in the rat. *Am J Physiol*. 1984; 247:H484-493.
 52. Neuwelt EA, Minna J, Frenkel E, Barnett PA, McCormick CI. Osmotic blood-brain barrier opening to IgM monoclonal antibody in the rat. *Am J Physiol*. 1986; 250:R875-883.
 53. Neuwelt EA, Specht HD, Barnett PA, Dahlborg SA, Miley A, Larson SM, Brown P, Eckerman KF, Hellstrom KE, Hellstrom I. Increased delivery of tumor-specific monoclonal antibodies to brain after osmotic blood-brain barrier modification in patients with melanoma metastatic to the central nervous system. *Neurosurgery*. 1987; 20:885-895.
 54. Neuwelt EA, Barnett PA, Hellstrom KE, Hellstrom I, McCormick CI, Ramsey FL. Effect of blood-brain barrier disruption on intact and fragmented monoclonal antibody localization in intracerebral lung carcinoma xenografts. *J Nucl Med*. 1994; 35:1831-1841.
 55. Remsen LG, McCormick CI, Roman-Goldstein S, Nilaver G, Weissleder R, Bogdanov A, Hellstrom I, Kroll RA, Neuwelt EA. MR of carcinoma-specific monoclonal antibody conjugated to monocrySTALLINE iron oxide nanoparticles: the potential for noninvasive diagnosis. *AJNR Am J Neuroradiol*. 1996; 17:411-418.
 56. Muldoon LL. Effect of antigenic heterogeneity on the efficacy of enhanced delivery of antibody-targeted chemotherapy in a human lung cancer intracerebral xenograft model in rats. *Neurosurgery*. 2003; 53:1406-1412; discussion 1412-1403.
 57. Jahnke K, Muldoon LL, Varallyay CG, Lewin SJ, Kraemer DF, Neuwelt EA. Bevacizumab and carboplatin increase survival and asymptomatic tumor volume in a glioma model. *Neuro Oncol*. 2009; 11:142-150.
 58. Muldoon LL, Lewin SJ, Dosa E, Kraemer DF, Pagel MA, Doolittle ND, Neuwelt EA. Imaging and therapy with rituximab anti-CD20 immunotherapy in an animal model of central nervous system lymphoma. *Clin Cancer Res*. 2011; 17:2207-2215.
 59. Lewis Phillips GD, Nishimura MC, Lacap JA, Kharbanda S, Mai E, Tien J, Malesky K, Williams SP, Marik J, Phillips HS. Trastuzumab uptake and its relation to efficacy in an animal model of HER2-positive breast cancer brain metastasis. *Breast Cancer Res Treat*. 2017.